Biophysical Journal Volume 96 April 2009 2709–2718

Sequence of Physical Changes to the Cell Membrane During Glucocorticoid-Induced Apoptosis in S49 Lymphoma Cells

Rachel W. Bailey, Thaothanh Nguyen, Leslie Robertson, Elizabeth Gibbons, Jennifer Nelson, Ryan E. Christensen, Jacob P. Bell, Allan M. Judd, and John D. Bell*
Department of Physiology and Developmental Biology, Brigham Young University, Provo, Utah

ABSTRACT During apoptosis, physical changes in the plasma membrane prepare the cell for clearance by phagocytes and hydrolysis by secretory phospholipase A_2 ($sPLA_2$). The relationships among these changes have not been adequately established, especially for hormone-stimulated apoptosis. This study addresses these issues for glucocorticoid-induced apoptosis in S49 lymphoma cells. Flow cytometry, microscopy, and fluorescence spectroscopy were used to assess merocyanine 540 emission, laurdan generalized polarization, phosphatidylserine exposure, caspase activation, and membrane permeability to propidium iodide in the absence and presence of $sPLA_2$. The earliest event observed was activation of cellular caspases. Results with membrane probes suggest that interlipid spacing also increases early during apoptosis and precedes transbilayer migration of phosphatidylserine, DNA fragmentation, and a general increase in lipid order associated with blebbing and dissolution of the cells. The activity of $sPLA_2$ appeared to be linked more to lipid spacing than to loss of membrane asymmetry. The early nature of some of these events and their ability to promote activity of a proinflammatory enzyme suggests the possibility of an inflammatory response during T-lymphocyte apoptosis.

INTRODUCTION

During apoptosis, structural changes occur in the plasma membrane that are necessary for clearance of expired cells by phagocytes. These changes include exposure of phosphatidylserine (PS) on the outer face of the membrane and budding of the membrane into microvesicles and apoptotic bodies (1–7). Additional observations suggest that modifications in the biophysical behavior of membrane lipids accompany these well-documented structural events. For example, several investigations have found that the ability of the fluorescent dye merocyanine 540 (MC540) to bind to cell membranes increases during apoptosis (1,2,8–11). Other studies have reported an increase in the ''fluidity'' of cell membranes during apoptosis initiated by certain agents (12–16). A recent investigation of rapid synchronized apoptosis stimulated by calcium ionophore suggested that membrane changes that may alter the researcher's perception of greater bilayer fluidity during cell death are complex (11). That study reported increased solvent accessibility to the membrane probe laurdan, but an absence of fluidity or lipid order changes detectable by diphenylhexatriene (DPH) anisotropy. Lastly, the membranes of some cells become susceptible to hydrolysis by secretory phospholipase A_2 ($sPLA_2$) during apoptosis (11,17,18).

The relationships among these various changes in membrane physical behavior have not been established. One logical hypothesis is that they are linked to exposure of PS. PS is normally a rare lipid on the extracellular side of cell membranes. During apoptosis, the lipid flips from the intracellular to the extracellular leaflet, presumably through the action of enzymes such as aminophospholipid translocase and scramblase (3,19,20). Elevation of intracellular calcium due to apoptotic signals inhibits the translocase, which normally transports PS and phosphatidylethanolamine to the interior side of the plasma membrane (3). At the same time, activation of scramblase by intracellular calcium causes random transbilayer migration of all glycerophospholipids, resulting in loss of membrane asymmetry (3,20). An increased negative surface charge would be expected to enhance interlipid spacing due to charge repulsion, which could account for the behavior detected by MC540, laurdan, and various probes reporting enhanced ''fluidity''. Likewise, $sPLA_2$ activity is greater toward synthetic membranes that contain anionic lipids (21–24), suggesting that exposure of PS may also account for the observation of greater susceptibility to hydrolysis of apoptotic membranes.

To examine this hypothesis, we conducted experiments to assess these various membrane behaviors and compare them with the exposure of PS during glucocorticoid-stimulated apoptosis in S49 lymphoma cells. These experiments presented special challenges because induction of apoptosis by steroid hormones initiates a time course of events that extends over several hours and varies in duration and speed from cell to cell (18,25). In preliminary studies, this problem was overcome by using a calcium ionophore to stimulate rapid synchronized apoptosis (11). However, whereas synchronization produced large ''all or none'' effects that were easy to measure, the speed of changes relative to the detection methods precluded the establishment of temporal relationships. Moreover, the use of an artificial inducer, such as calcium ionophore, limits confidence in the physiological relevance of the conclusions. In this study, we used

Submitted October 17, 2008, and accepted for publication December 18, 2008.

*Correspondence: john_bell@byu.edu

Editor: Arup Chakraborty.

0006-3495/09/04/2709/10 $2.00

doi: 10.1016/j.bpj.2008.12.3925

fluorescence spectroscopy, two-photon microscopy, and flow cytometry to better establish temporal relationships during apoptosis induced by the glucocorticoid dexamethasone (dex). The results compelled us to reject the hypothesis and conclude that subtle membrane changes occur during apoptosis that precede PS exposure and may be responsible for regulating the membrane's vulnerability to enzymatic hydrolysis.

MATERIALS AND METHODS

See description in the Supporting Material.

RESULTS

Physical changes in the cell membrane

Probes of lipid order, fluidity, and hydration

Initial attempts to monitor laurdan generalized polarization (GP) by spectroscopy revealed no changes in the dex-treated samples (data not shown). There are several possible explanations for this observation: there may be no changes during dex-stimulated apoptosis, the changes may be very subtle, cells at different points along the apoptotic continuum probably coexist in the same sample, and/or laurdan GP may sequentially change in more than one direction from the initial level.

To explore these possibilities, we visualized the spatial distribution of laurdan GP values in dex-treated cell membranes by means of two-photon excitation microscopy. This approach allowed laurdan GP to be calculated for individual cells and not averaged for entire samples as in the cuvette. Twenty images were collected for each experiment to obtain a representative sample. During the collection and analysis of these images, one major observation was made: cells could be classified into three distinct categories based on the spatial pattern of the GP values. We focused on the perimeter of the cell in an effort to confine our interpretations to the plasma membrane. For convenience of presentation, we defined the three categories as 1), "ring" (see cell 1 in Fig. 1 *A*), referring to the contrasting higher GP values that characterize the cell perimeter; 2), "mixed" (cell 2 in Fig. 1 *C*), referring to the greater heterogeneity of GP values along the perimeter and the absence of the high-GP ring; and 3), "red" (cell 3 in Fig. 1 *D*), referring to the homogeneous high-GP values of the entire cell. The divisions among categories were evident from both the GP values (of the whole cell and the interior) and visual sorting. The numerical distinctions for each category are summarized in Table S1 in the Supporting Material. The cell populations were initially composed mostly of ring cells with a few mixed or red cells. As apoptosis progressed to ~40% dead, there was a rise in mixed cells concurrent with a reduction in the proportion of ring cells. Finally, when the population reached 75% dead, the mixed and ring cells decreased, and red became the dominant pattern (displayed in Fig. 1 *E*).

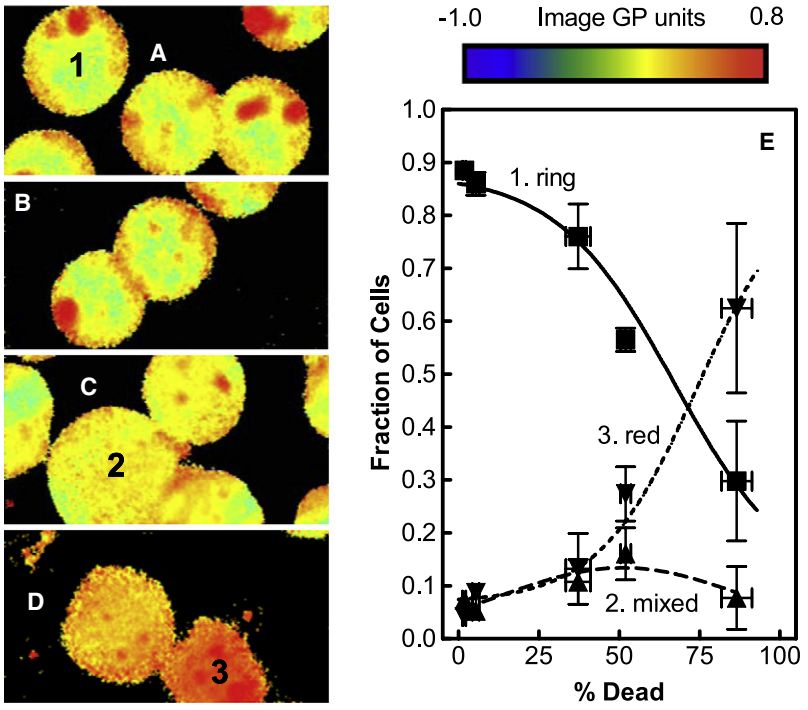

FIGURE 1 Progression of the pattern of laurdan GP across the cell in response to dex treatment. Cells were incubated with dimethylsulfoxide (DMSO) for 24 h (*A*) or with dex for 6 h (*B*), 24 h (*C*), or 48 h (*D*). They were then labeled with laurdan, and images of laurdan GP were obtained by two-photon excitation microscopy. Cells were classified into three visual categories: ring (e.g., cell 1), mixed (e.g., cell 2), or red (e.g., cell 3) (see Table S1 for quantitative classification). (*E*) The experiments shown in *A–D* were repeated at various incubation times with DMSO or dex (6–48 h, 6 h increments). The percentage of dead cells (by PI uptake) was quantified in parallel for each sample to calibrate progression through apoptosis (displayed on the abscissa). The fraction of the total population in each category (ring: *squares* and *solid curve*; mixed: *triangles* and *dashed curve*; red: *inverted triangles* and *dotted curve*) was counted from the images (20 images with an average of 5.1 cells per image were analyzed for each of the 23 independent samples). The sets of individual data points were fit to Eq. S5 by nonlinear regression before grouping (mean ± SE in both dimensions, $n = 3–6$) for the ring and red populations. The DMSO and dex samples were both included in the regression, allowing the control group to function as an anchor near the origin for the fit. Both are also pooled together in the figure (average % dead ± SD in DMSO group = 8% ± 12%, $n = 11$; in dex group = 52% ± 25%, $n = 12$; cell fractions ± SD in each category for the DMSO group were ring: 0.84 ± 0.11; mixed: 0.06 ± 0.03; and red: 0.10 ± 0.12). The curve for the mixed population was obtained by subtracting the other two curves from a constant of 1.0.

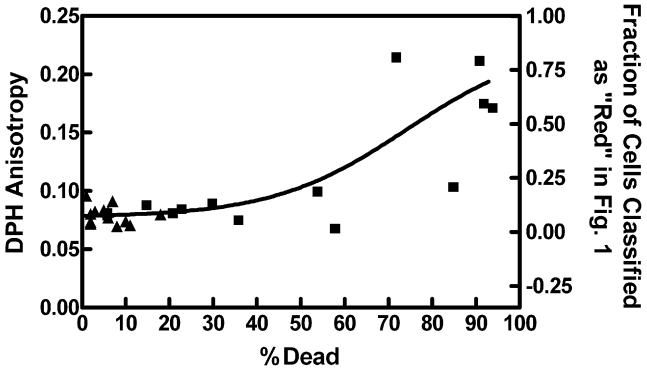

FIGURE 2 Effect of dex treatment on DPH anisotropy. Samples were treated with DMSO (*triangles*) or dex (*squares*) for various times between 0 and 48 h. Data are plotted as a function of apoptosis progression (percentage of dead cells based on trypan blue uptake). The curve is the same as the dotted nonlinear regression curve from Fig. 1 *E* (red population). The difference between DMSO and dex samples treated for 48 h was statistically significant by paired *t*-test ($p = .001$, $n = 4$).

As shown in Fig. 2, DPH anisotropy was also elevated in this high-laurdan GP population.

Merocyanine 540

The timing of changes in MC540 fluorescence intensity was evaluated by means of spectroscopy and flow cytometry. As shown in Fig. 3 *A*, treatment of S49 cells for 24 h with dex increased the intensity of MC540 emission ~2-fold (*solid gray curve* compared to *solid black curve*). As explained in Materials and Methods, samples were additionally treated for 10 min with ionomycin to establish the maximum MC540 intensity for each sample (*dashed curves*). The experiment of Fig. 3 *A* was repeated for various incubation times with either DMSO or dex (see figure legend). The data were quantified as the fraction of cells displaying high-intensity MC540 fluorescence (see Eq. S2, *squares*). Fig. 3*B* illustrates the result of this analysis: the fraction of MC540-positive cells displayed a sigmoid function as apoptosis progressed (indicated as % dead by trypan blue). Repetition of the experiment by flow cytometry yielded identical results (Fig. 3 *B*, *triangles*, midpoint ± 95% confidence interval (CI) of the time course corresponded to 36.3% ± 2.6% dead).

Interpretation of the data in Fig. 3 depends on the assumption that the observed MC540 fluorescence corresponds to staining confined to the cell membrane. This assumption was tested by confocal microscopy (see Figs. S1 and S2, with associated text). These experiments demonstrated that MC540 stains only the plasma membrane during the first one-fourth of the apoptosis time course in S49 cells, but the cell membranes become permeable to the dye as apoptosis progresses further. Quantitative analysis of the micrographs also suggested that the increase in MC540 intensity during apoptosis reflects a change in the lateral distribution of the dye along the plane of the bilayer.

PS exposure

Transbilayer movement of PS to the outer leaflet was evaluated by means of flow cytometry. Cells treated with dex or DMSO were mixed with fluorescein isothiocyanate-annexin (FITC-annexin), a fluorescently labeled protein that binds to exposed PS (26). Fig. 4 displays the fraction of cells that stain positive for fluorescein (*symbols* and *solid curve*) and therefore presumably bind to annexin (f_F, Eq. S4) as a function of progression through apoptosis. The observed midpoint for apparent PS exposure was 60.4% ± 4.8% (mean ± 95% CI) dead.

The purpose of assessing annexin binding was to test the hypothesis that other changes in the membrane observed during apoptosis might be linked to the exposure of PS on the surface of cells, as suggested previously (1,2,6,10, 21–24,27,28). The dashed curve in Fig. 4 displays the relationship obtained by nonlinear regression of the MC540 data from Fig. 3. There was a detectable displacement between the two sets of observations: cells stained positive for MC540 before the exposure of PS. The difference between the two data sets was statistically significant because the 95% CIs for the midpoints did not overlap (34–39% for MC540 and 56–65% for FITC-annexin).

An important caveat for interpreting the results shown in Fig. 4 is the observation in Fig. S1 that cells stain internally

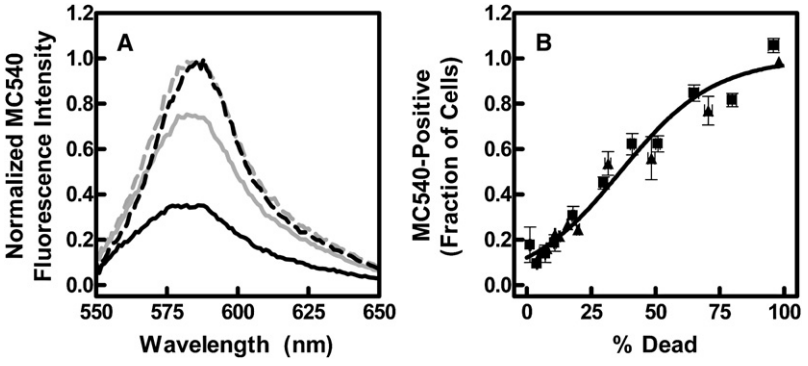

FIGURE 3 Effect of dex treatment on MC540 fluorescence intensity. (*A*) Emission spectra of MC540 bound to cells treated for 24 h with DMSO (*black*) or dex (*gray*) before (*solid curves*) or after 10 min additional incubation with ionomycin (*dashed curves*). Spectra were normalized to their respective maxima in the dashed curves. (*B*) MC540 response as a function of apoptosis progression (percentage of dead cells based on trypan blue uptake). The experiments of panel *A* were repeated for various incubation periods with dex or DMSO (up to 48 h). The fraction of cells positive for high-intensity MC540 staining was estimated as explained in Materials and Methods (Eq. S2, *squares*). Triangles represent similar experiments assayed by flow cytometry (quantified using Eq. S3). Data were fit to Eq. S5 before grouping (mean ± SE in both dimensions, $n = 4$–20). As in Fig. 1 *E*, data from DMSO and dex-treated samples were pooled (spectroscopy—DMSO average % dead ± SD = 7% ± 8%, $n = 59$; dex: 49% ± 28%, $n = 60$; flow cytometry—DMSO: 13% ± 8%, $n = 34$; dex: 28% ± 21%, $n = 34$; DMSO group MC540-positive fraction ± SD—spectroscopy: 0.14 ± 0.21 and flow cytometry: 0.22 ± 0.15).

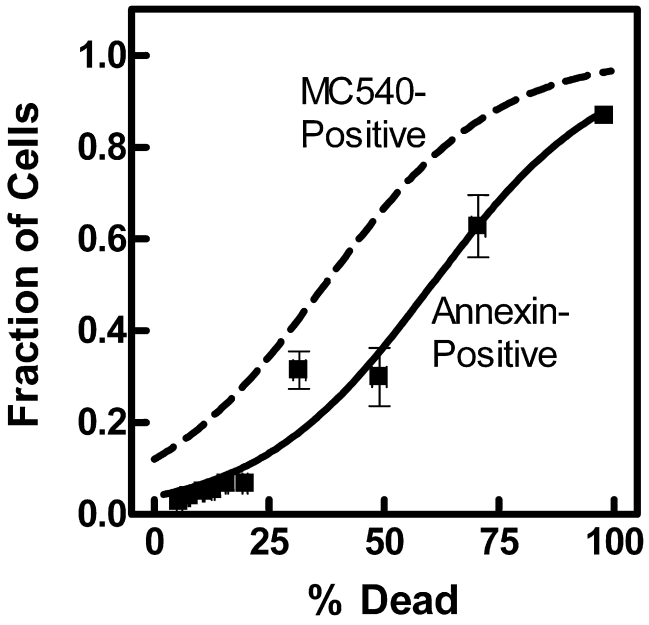

FIGURE 4 Comparison of dex-stimulated changes in annexin binding and MC540 fluorescence. Annexin binding was assessed by flow cytometry and quantified using Eq. S4. Data were fit to Eq. S5 before grouping (*solid curve*; mean ± SE in both dimensions, $n = 1$–9 per datum). The dashed curve represents the nonlinear regression curve from Fig. 3 *B* (fraction of cells positive for high-intensity MC540 fluorescence). As in Fig. 1 *E*, data from DMSO and dex-treated samples were pooled (DMSO average % dead ± SD = 12% ± 8%, $n = 30$; dex: 28% ± 22%, $n = 31$; DMSO annexin-positve fraction ± SD: 0.08 ± 0.11).

with MC540 as apoptosis progresses. To avoid this confounding factor, we utilized a second analysis method focusing on the first 8 h (~1/6) of the apoptosis time course, during which interval the staining with MC540 appeared to be confined to the cell membrane. For this second analysis, all data were gathered from cells that had been incubated simultaneously with both MC540 and FITC-annexin. The analysis was designed for high sensitivity because we expected that differences between events would be subtle at early time points (too subtle for conventional two-color flow cytometry analysis). The results of this analysis are shown in Figs. S3 and S4 (with associated text) and confirm the interpretation that changes in MC540 fluorescence precede PS exposure.

Time course of $sPLA_2$ susceptibility

The percentage of S49 cells with plasma membranes susceptible to hydrolysis by $sPLA_2$ was evaluated by monitoring the intensity of propidium iodide (PI) fluorescence as a function of time. The rationale for using PI was based on the concept that cell membranes are impermeable to the dye unless compromised either by hydrolysis or by cell death. When membranes become permeable, the dye enters the nucleus and binds to DNA, resulting in a substantial increase in fluorescence intensity. Thus, comparison of PI fluorescence intensity before and after addition of $sPLA_2$ functions as a convenient assay to determine the proportion of cells that are alive (i.e., initially exclude the dye) but susceptible to the enzyme (i.e., incorporate the dye upon addition of $sPLA_2$) (29).

A sample time course of PI fluorescence is illustrated in Fig. 5 *A*. PI was added at point a, and $sPLA_2$ was added after equilibration with the probe (point b). Once the fluorescence signal stabilized after enzyme addition, ionomycin was added (point c). The purpose of including ionomycin was to render any resistant cells remaining in the population susceptible, providing a measure of maximal PI fluorescence intensity that corresponded to 100% of cells staining with the dye. The ability of ionomycin to induce maximal susceptibility was confirmed by repeating the assay with detergent added after ionomycin (data not shown).

Fig. 5 *B* shows the temporal progression of various populations of cells identified from the time courses. These populations were defined and calculated as follows:

1. Cells that are already dead take up the dye immediately before addition of either $sPLA_2$ or ionomycin. These are designated ''initially permeable'' (*red symbols* and *curve* in Fig. 5) and were calculated as the intensity at point a subtracted from that at point b, and then normalized to the total fluorescence change (difference between point e and point a).
2. Cells that incorporate PI upon addition of $sPLA_2$ were identified as ''alive, but susceptible'' to $sPLA_2$ (*brown* in Fig. 5) and calculated as point c − point b (and again normalized to point e − point a).
3. Since the membranes of both of the previous two populations are hydrolyzed by $sPLA_2$ (29), the sum of the two is denoted as ''early susceptible'' (*green* in Fig. 5).
4. The fraction of cells with ''fragmented DNA'' was estimated by comparing PI intensity after ionomycin between control and dex-treated samples (*violet* in Fig. 5, point e − point f, normalized; see Materials and Methods for details).
5. The total of all cells susceptible to $sPLA_2$ (*blue* in Fig. 5) was calculated as the sum of the first, second, and fourth populations.

The relationships among the ''initially permeable'' (*red*), ''alive but susceptible'' (*brown*), and ''early susceptible'' (*green*) populations and the laurdan ''mixed'' population from Fig. 1 (*black curve*) are considered in Fig. 5 *C*. Similar considerations are shown between MC540 fluorescence (*black dashed curve*) or PS exposure (FITC-annexin binding, *black dotted curve*) from Figs. 3 and 4 and the ''total susceptible'' (*blue*) or ''fragmented DNA'' (*violet*) populations in Fig. 5, *D* and *E*.

Several temporal relationships apparent in Fig. 5 were validated by comparing the midpoints and 95% CIs for the progression of the various events during apoptosis obtained from the nonlinear regressions (Table 1). For example, emergence of the intermediate population of membrane structures

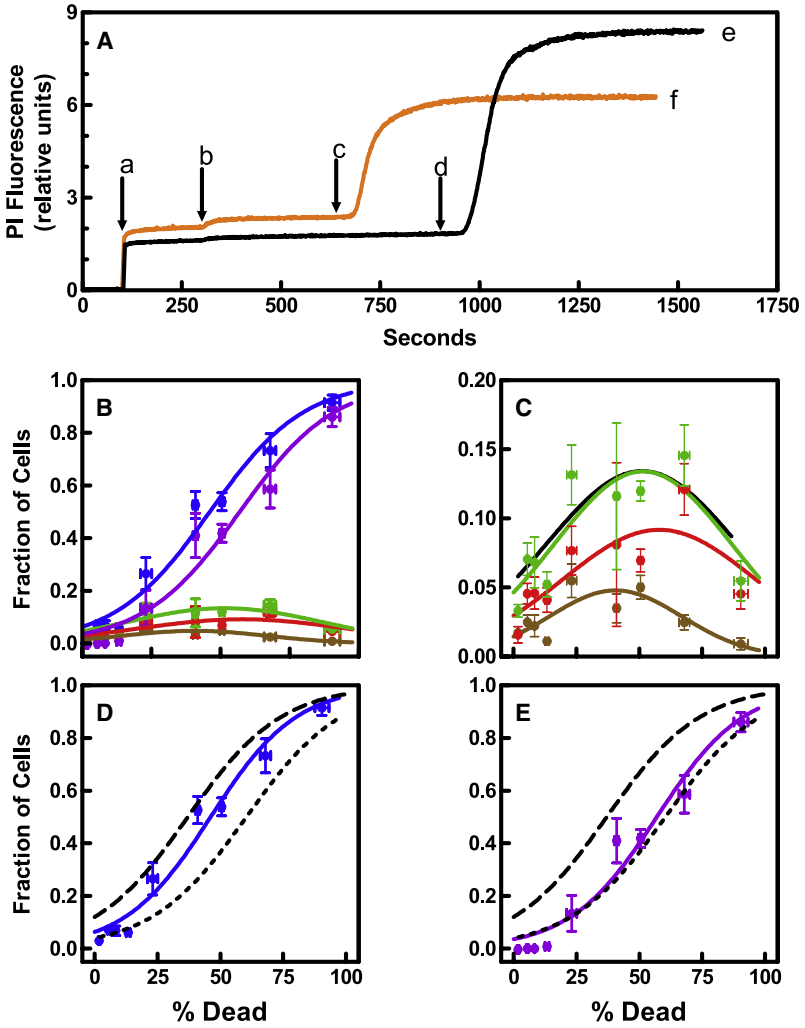

FIGURE 5 Temporal comparison of dex-stimulated susceptibility to $sPLA_2$ hydrolysis with laurdan GP, MC540 fluorescence, and annexin binding. (*A*) Representative time course of PI fluorescence. Cells were incubated with DMSO (*black curve*) or dex (*orange curve*) for 17 h. PI was added at point a, $sPLA_2$ at point b, and ionomycin at point c (dex) or d (DMSO). (*B*) The experiments of panel *A* were repeated for various incubation periods with dex or DMSO (up to 48 h). The populations of cells alive but susceptible to $sPLA_2$ (*brown circles*, intensity at point c subtracted from that at point b), initially permeable to PI (*red circles*, point b − point a), displaying early susceptibility to $sPLA_2$ (*green circles*, point c − point a), or containing fragmented DNA (violet circles, point e – point f) were calculated from the time course data and plotted as a function of the percentage of dead cells in each sample (trypan blue uptake). The blue circles are the sums of the corresponding green and violet data. The data were normalized to the maximum response in control samples (point e − point a) to obtain the fractional response. Before grouping, data showing a transient maximum were fit to an arbitrary function, and the rest were fit with Eq. S5 (mean ± SE in both dimensions, n = 6–10). As in Fig. 1 *E*, data from DMSO and dex-treated samples were pooled (DMSO average % dead ± SD = 9 ± 8%, n = 35; dex: 52 ± 24%, n = 37; DMSO initially permeable fraction: 0.06 ± 0.07; DMSO alive, susceptible fraction: 0.02 ± 0.02; DMSO early susceptible fraction: 0.08 ± 0.08). Panel *C* shows the "alive but susceptible" (*brown*), "initially permeable" (*red*), and "early susceptibility" (*green*) populations from panel *B* superimposed on the regression curve (*black*) from the mixed laurdan population in Fig. 1 *E*. In panels *D* and *E* the regression curves from Fig. 3 (MC540, *dashed black curve*) and Fig. 4 (annexin binding, *dotted black curve*) were superimposed with the "total susceptibility" data (*blue*) or "fragmented DNA" data (*violet*) from panel *B*.

detected by laurdan (the "mixed" subpopulation in Fig. 1) coincided exactly with the subpopulation of cells displaying early susceptibility to $sPLA_2$ (*green* and *black curves* in Fig. 5 *C*). The population of all cells susceptible to $sPLA_2$ appeared earlier than the population that stained positive for FITC-annexin, and later than the changes in MC540 fluorescence (Fig. 5 *D*). Finally, annexin binding coincided with DNA fragmentation (Fig. 5 *E*).

Fig. 6 shows that susceptibility to $sPLA_2$, like other, better-established apoptotic events, depends on the involvement of cellular caspases. Fig. 6 *A* displays the progression of caspase activation assayed with the fluorescently labeled general caspase inhibitor FAM-VAD-fmk (*solid curve*; the *dashed* and *dotted curves* represent the progression of MC540 fluorescence intensity and annexin binding from Figs. 3 and 4). Table 1 demonstrates that this event was the earliest among those measured (midpoint ± 95% CI: 21.8 ± 5.4%). As shown in Fig. 6 *B*, general inhibition of caspases (*open circles*) reduced the amount of hydrolysis of dex-treated cells by $sPLA_2$.

DISCUSSION

The primary objective of this study was to identify the temporal relationships among various physical changes associated with the cell membrane during glucocorticoid-stimulated apoptosis. Several physical changes associated with apoptosis were reported previously. Experiments with various fluorescent probes suggested that the fluidity of cell membranes increases during apoptosis (12–14). Likewise, MC540 fluorescence appears to be sensitive to apoptosis (1,2,8–11). In a recent study, laurdan was also shown to be a candidate for detecting apoptotic changes in the cell membrane (11). Although previous reports established the concept that membrane properties change during apoptosis, they were unable to identify clear temporal or mechanistic relationships. This point is especially true for apoptosis initiated by hormones. By assessing temporal relationships during glucocorticoid-stimulated apoptosis, we were able to address certain proposed mechanisms. Table 2 lists the hypotheses considered and the relevant conclusions derived from the observations of this study.

TABLE 1 Midpoints with 95% CIs for the various events detailed in Figs. 1 and 3–6

		Parameters		
Measurement	Figure	Midpoint (% dead)	CI lower limit	CI upper limit
1. Caspase activation	6 *A*, *solid*	21.8	16.4	27.2
2. Cells with high intensity MC540 staining	3 *B*	36.3	33.7	38.9
3. Cells alive but susceptible to $sPLA_2$	5 *B*, *brown*	40.6	33.5	47.6
4. Laurdan mixed population	1 *E*, *dashed*	51.1	25.8	76.5
5. Early susceptibility to $sPLA_2$ (sum of rows 3 and 7)	5 *B*, *green*	51.5	41.4	61.5
6. Total susceptibility to $sPLA_2$ (sum of rows 5 and 8)	5 *B*, *blue*	46.1	43.4	48.9
7. Cells initially permeable to PI	5 *B*, *red*	57.9	40.1	75.8
8. Cells with fragmented DNA	5 *B*, *violet*	57.0	53.2	60.7
9. FITC-annexin binding	4, *solid*	60.4	55.6	65.2
10. Laurdan red population	1 *E*, *dotted*	74.2	63.3	85.1

The events are listed in their estimated temporal sequence during dex-stimulated apoptosis. Parameter values were obtained by nonlinear regression as explained in the legends to the referenced figures.

Micrographs of laurdan GP revealed two distinct populations that emerge as a result of glucocorticoid stimulation: one with decreased GP values (i.e., ''mixed'' in Fig. 1) and one with increased GP values (i.e., ''red'' in Fig. 1). The fact that the hydrated mixed population appeared and disappeared over the course of apoptosis suggests that it represents an intermediate state between the baseline ring and high-GP red states. This interpretation is reinforced by a previous investigation that also reported a shift from ring to mixed in S49 cells undergoing ionophore-stimulated apoptosis (11). In that study, DPH anisotropy was assayed under the same conditions but no changes were observed, suggesting that the reduction in laurdan GP reflects increased water penetration into the bilayer without a concurrent change in lipid fluidity or order. In contrast, the high-GP red population that emerged late during dex-stimulated apoptosis was accompanied by a detectable increase in DPH anisotropy, suggesting that this cell population contains membranes with increased order (Fig. 2). Moreover, visual inspection of the micrographs that contain large numbers of red cells suggests that emergence of this membrane state corresponds to blebbing and other fragmentation of the cell membrane (e.g., Fig. 1 *D*).

A previous assessment of laurdan GP values during ionophore-induced apoptosis indicated that coincident elevation of MC540 fluorescence intensity may reflect an increase in headgroup spacing of membrane phospholipids (11). If the transient decrease in laurdan GP and the increase in MC540 emission represent the same membrane event, they should happen concurrently. The differences in the shape of the progression of the two events (temporary versus persistent) make it difficult to directly compare the timing of the events. Nevertheless, as summarized in the first and third rows of Table 1, the midpoint of the MC540 fluorescence increase cannot be distinguished statistically from the zenith of the laurdan GP profile, suggesting the possibility that the two fluorescence observations are concurrent. The question might well be raised as to how the two observations could portray the same molecular event, since the curve shapes are so different. However, as illustrated in Fig. S1, the initial change in MC540 fluorescence is also temporary as the cells progress to a state in which the membrane becomes permeable to the dye. The only difference then in the profile shapes is that flow cytometry and spectroscopy do not distinguish the intermediate and final states detected by MC540, whereas the two behave

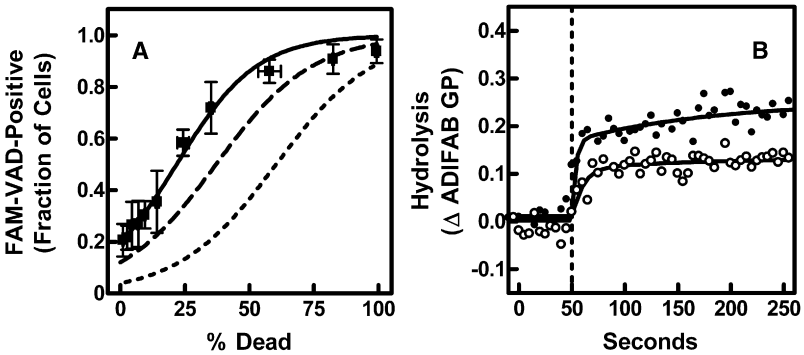

FIGURE 6 Relationship between caspase activation and membrane changes. (*A*) FAM-VAD-fmk binding was assessed by flow cytometry and quantified with Eq. S3 as described in Materials and Methods for samples incubated for various periods of time with dex or DMSO (up to 48 h). Data were fit to Eq. S5 before grouping (*solid curve*, mean ± SE in both dimensions, $n = 2$–10 per datum). As in Fig. 1 *E*, data from DMSO and dex-treated samples were pooled (DMSO average % dead ± SD = 4 ± 3%, $n = 29$; dex: 31 ± 31%, $n = 30$; DMSO FAM-VAD-positive fraction ± SD: 0.25 ± 0.21). The dashed curve represents the nonlinear regression curve from Fig. 3 *B* (fraction of cells positive for high-intensity MC540 fluorescence). The dotted curve represents the nonlinear regression curve from Fig. 4 (fraction of cells positive for FITC-annexin staining). (*B*) Time course of hydrolysis assessed by the GP of acrylodan-labeled fatty acid binding protein (ADIFAB). Cells were incubated with dex for 24 h with (*open circles*) or without (*solid circles*) Z-VAD-fmk (added concurrently with dex). The changes in GP values before and after addition of $sPLA_2$ (*dotted line*) were fit to an arbitrary function.

TABLE 2 Hypotheses addressed in this study

Hypothesis	Reference	Conclusion from this study
Laurdan GP and MC540 fluorescence reflect the same membrane event: increased interlipid spacing.	(11)	supported
Increased interlipid spacing increases the susceptibility of the membrane to hydrolysis by $sPLA_2$.	(11)	supported
Increased MC540 fluorescence is caused by exposure of PS on the external membrane face.	(1,2,6,10,27)	rejected
Increased susceptibility of the membrane to $sPLA_2$ is caused by PS exposure.	(21–24,28)	rejected

differently with respect to laurdan GP (i.e., mixed versus red populations).

A quantitative analysis of the confocal microscopy data suggests that lipid spacing is not uniform along the plasma membrane (Fig. S2). Moreover, the level of heterogeneity appeared to increase during apoptosis. If the rise in total MC540 fluorescence intensity in response to dex or ionomycin treatment were due solely to increased probe binding, the shape of the distribution of pixel intensity would not have changed. Instead, the mode of the distribution would simply have moved to a higher value along the abscissa with no change in shape.

It has been hypothesized that the apparent increase in spacing among lipids in apoptotic cells is merely a direct consequence of the translocation of PS to the outer leaflet. Previous studies found a correlation between these two events in various cell types (9,10,27). Moreover, MC540 binding has been used as an assay of PS exposure (1,6). In contrast, in a premyeloid leukocyte line (32D cells), the PS exposure occurred earlier than MC540 fluorescence changes (9). However, the resolution of the data in these studies is insufficient to reveal small temporal displacements. Furthermore, the studies employed too few experimental samples to test the statistical significance of the observations. In contrast, the experiments shown in Figs. 4 and S4 contain sufficient data of adequate resolution to address the relationship between these two events. The results in both cases argue that increases in MC540 fluorescence precede the translocation of PS to the outer membrane leaflet. A comparison of rows 1 and 8 of Table 1 reveals that the 95% CIs for the midpoints of the two events are far from overlapping, suggesting high statistical significance. Thus, the data do not support a causal relationship between PS exposure and MC540 fluorescence. Alternatively, the two events are either independent or parallel with a common inducer. This conclusion would explain the cell type-dependent disparity observed in a previous study (9). Our interpretation of these results is not intended to indicate that exposure of PS would not or could not increase the binding and/or fluorescence intensity of MC540. Instead, it simply means that changes in MC540 fluorescence in apoptotic cells appear not to require or necessarily imply loss of the natural membrane asymmetry of PS.

PS exposure also appeared to occur too late during apoptosis to cause the initial onset of membrane susceptibility to $sPLA_2$ in S49 cells (see Fig. 5 and Table 1). This issue has been somewhat controversial in the past. On the one hand, there is a general consensus that a negative charge in the membrane (such as would be provided by the anionic PS) does influence the activity of most isoforms of $sPLA_2$ in a positive way (21–24,28,30,31). However, whether the presence or absence of such a charge is the primary or sole determinant of the extent to which cell membranes are vulnerable to $sPLA_2$ has been less certain (11,18,32,33). Although a few lines of evidence have suggested that PS exposure may not be a requirement for membranes to be attacked by $sPLA_2$ (18,32), this study removes any ambiguity by including an experimental design in which hydrolysis and PS exposure were assayed in the same samples (i.e., every sample assayed by flow cytometry was also assayed for $sPLA_2$-stimulated PI uptake in parallel aliquots of the same sample). Of interest, the exposure of PS in S49 cells was concurrent with the diminution in maximum PI staining associated with DNA fragmentation (Fig. 5 *E*; also see Materials and Methods).

In contrast to the exposure of PS, the somewhat earlier changes in the membrane detected by laurdan and MC540 appeared to correspond temporally with the ability of $sPLA_2$ to hydrolyze the membrane. This temporal correlation is strongest when one focuses attention on those cells with the earliest onset of susceptibility to $sPLA_2$ (Fig. 5, *C* and *D*; compare the first four rows of Table 1).

We hypothesize that the membrane event(s) detected by laurdan or MC540 cause the elevation in $sPLA_2$ activity during apoptosis. This idea is substantiated by several prior observations. For example, many studies have established that the enzyme is extremely sensitive to certain membrane properties assessed and manipulated in artificial bilayers, such as the phase of the lipids, the lateral distribution of membrane components, and the strength of neighbor-neighbor interactions (21,30,31,34–36). More recently, a few studies have attempted to link changes in lipid packing to the activity of $sPLA_2$ toward intact cells (11,37,38). The concept is that diminished interactions among neighboring phospholipids would facilitate the vertical migration of phospholipids into the active site of $sPLA_2$ adsorbed to the membrane surface (11,30,37,39). Nevertheless, the methods previously used to induce alterations in cell membrane lipid packing act so rapidly that it has been difficult to test this hypothesis and to distinguish contributions from other possible mechanisms, such as PS exposure (11,37,38). This problem was resolved by the experiments presented here because of the temporal resolution that was possible during the prolonged time course of hormone-induced apoptosis. Using this resolution, we were able to reject the hypothesis that PS exposure is required (see above), but the hypothetical relationship among laurdan GP, MC540 emission intensity, and $sPLA_2$ activity was supported.

A membrane change often associated with ''late apoptosis'' is the loss of membrane integrity. In our experiments, this loss was manifested by internalization of MC540 (Fig. S1) and, more conventionally, by the uptake of PI before addition of $sPLA_2$. As shown in Table 1, the loss of membrane integrity assayed with PI staining occurred later than the changes detected by laurdan and MC540, and appeared to be grouped with DNA fragmentation and exposure of PS. The laurdan and DPH (Figs. 1 and 2) data suggest that the membrane acquires a highly ordered state (i.e., the red population) at this point during apoptosis. Hence, the increased permeability to PI probably reflects gross breaks in the membrane during blebbing and microvesicle release rather than enhanced permeability at the molecular scale.

Much work is still needed to address all of the mechanistic links between glucocorticoid signaling and the observed membrane changes. Based on the data of Fig. 6, the typical activation of caspases appears to be part of the process. Moreover, this activation was an early event consistent with the expected role of these enzymes as upstream participants in the apoptotic pathway (40). More specifically, the data of Fig. 6 *B* indicate that the induction of membrane susceptibility to $sPLA_2$ is at least partially caspase-dependent. Intermediate steps between caspase activation and biophysical changes at the membrane remain mostly unexplored, but may include elements such as cytoskeletal alterations, changes in lipid clustering or distribution, and variations in lipid and/or protein content of the membrane. Several studies have suggested that cytoskeleton alterations play an important role in apoptosis (41–43). Moreover, the activity of intracellular phospholipases A_2, C, and D all appear to be influenced by changes in cytoskeletal elements (44–46). The activation of these hydrolytic enzymes could then alter membrane properties, leading to vulnerability to $sPLA_2$, although evidence does not support this idea for intracellular phospholipase A_2 in S49 cells (47). Alternatively, cytoskeletal rearrangement or disruption could certainly affect membrane rigidity and lipid membrane domains directly, as suggested by a few studies with fluorescent membrane probes (48,49). The increased heterogeneity of MC540 fluorescence intensity detected by confocal microscopy (Fig. S2) suggests that such redistribution is a realistic possibility. Moreover, elevated membrane concentrations of ceramide commonly accompany apoptosis (50). This change in membrane lipid composition is a strong candidate for altering the average physical properties of the membrane as well as the distribution of lipid domains (16,51,52).

In summary, we propose the following scheme as a general hypothesis for the sequence of membrane events associated with glucocorticoid-stimulated apoptosis in lymphocytes:

1. Activation of caspases.
2. Subtle changes involving interactions among membrane lipids that result in an increase in interlipid spacing, increased hydration, and susceptibility to the action of $sPLA_2$. It is likely that, depending on the cell type, the enhanced membrane fluidity that has been reported corresponds to this cluster of events.
3. Exposure of PS. This event appears to be independent of event 1 but, depending on the cell type, may occur concurrently with it or even precede it.
4. Increased membrane permeability to dyes such as MC540 or PI.
5. Increased membrane order. This event appears to correspond to membrane blebbing and fragmentation.

This scheme has at least one important physiological implication. Conventional wisdom dictates that the purpose of PS exposure and packaging of cellular remnants into apoptotic bodies is to facilitate phagocytosis by macrophages, thereby mitigating an inflammatory response (53,54). However, since the membrane changes that render the cell susceptible to $sPLA_2$ may precede those recognized by macrophages, it appears that an inflammatory response is still a potential issue for apoptotic cells, at least under certain circumstances.

SUPPORTING MATERIAL

Five equations, one table, and four figures are available at http://www.biophysj.org/biophysj/supplemental/S0006-3495 (09)00393-2.

We thank Enrico Gratton, Theodore Hazlett, Susana Sanchez, Oliver Holub, and the Laboratory for Fluorescence Dynamics (Irvine, CA) for providing facilities and expertise for the two-photon experiments. We also thank Erin Olson, Celestine Yeung, Mara Whitworth, Katalyn Griffith, Michael Streeter, Ashley Warcup, and Brian Stott for providing technical assistance. This work was supported by the National Institutes of Health (GM073997).

REFERENCES

1. Fadok, V. A., D. R. Voelker, P. A. Campbell, J. J. Cohen, D. L. Bratton, et al. 1992. Exposure of phosphatidylserine on the surface of apoptotic lymphocytes triggers specific recognition and removal by macrophages. *J. Immunol.* 148:2207–2216.
2. Ashman, R. F., D. Peckham, S. Alhasan, and L. L. Stunz. 1995. Membrane unpacking and the rapid disposal of apoptotic cells. *Immunol. Lett.* 48:159–166.
3. Verhoven, B., R. A. Schlegel, and P. Williamson. 1995. Mechanisms of phosphatidylserine exposure, a phagocyte recognition signal, on apoptotic T lymphocytes. *J. Exp. Med.* 182:1597–1601.
4. Schlegel, R. A., M. Callahan, S. Krahling, D. Pradhan, and P. Williamson. 1996. Mechanisms for recognition and phagocytosis of apoptotic lymphocytes by macrophages. *Adv. Exp. Med. Biol.* 406:21–28.
5. Krahling, S., M. K. Callahan, P. Williamson, and R. A. Schlegel. 1999. Exposure of phosphatidylserine is a general feature in the phagocytosis of apoptotic lymphocytes by macrophages. *Cell Death Differ.* 6:183–189.
6. Callahan, M. K., P. Williamson, and R. A. Schlegel. 2000. Surface expression of phosphatidylserine on macrophages is required for phagocytosis of apoptotic thymocytes. *Cell Death Differ.* 7:645–653.
7. Fadeel, B., and S. Orrenius. 2005. Apoptosis: a basic biological phenomenon with wide-ranging implications in human disease. *J. Intern. Med.* 258:479–517.
8. Mower, D. A., Jr., D. W. Peckham, V. A. Illera, J. K. Fishbaugh, L. L. Stunz, et al. 1994. Decreased membrane phospholipid packing and decreased cell size precede DNA cleavage in mature mouse B cell apoptosis. *J. Immunol.* 152:4832–4842.

9. Hess, K. L., J. D. Johnson, and J. M. Cook-Mills. 2001. Different orders for acquisition of apoptotic characteristics by leukocytes. *J. Leukoc. Biol.* 70:405–412.
10. Laakko, T., L. King, and P. Fraker. 2002. Versatility of merocyanine 540 for the flow cytometric detection of apoptosis in human and murine cells. *J. Immunol. Methods.* 261:129–139.
11. Bailey, R. W., E. D. Olson, M. P. Vu, T. J. Brueseke, L. Robertson, et al. 2007. Relationship between membrane physical properties and secretory phospholipase A2 hydrolysis kinetics in S49 cells during ionophore-induced apoptosis. *Biophys. J.* 93:2350–2362.
12. Jourd'heuil, D., A. Aspinall, J. D. Reynolds, and J. B. Meddings. 1996. Membrane fluidity increases during apoptosis of sheep ileal Peyer's patch B cells. *Can. J. Physiol. Pharmacol.* 74:706–711.
13. Fujimoto, K., C. Iwasaki, H. Kawaguchi, E. Yasugi, and M. Oshima. 1999. Cell membrane dynamics and the induction of apoptosis by lipid compounds. *FEBS Lett.* 446:113–116.
14. Raghavendra, P. B., Y. Sreenivasan, and S. K. Manna. 2007. Oleandrin induces apoptosis in human, but not in murine cells: dephosphorylation of Akt, expression of FasL, and alteration of membrane fluidity. *Mol. Immunol.* 44:2292–2302.
15. Baritaki, S., S. Apostolakis, P. Kanellou, M. T. Dimanche-Boitrel, D. A. Spandidos, et al. 2007. Reversal of tumor resistance to apoptotic stimuli by alteration of membrane fluidity: therapeutic implications. *Adv. Cancer Res.* 98:149–190.
16. Moulin, M., S. Carpentier, T. Levade, and A. P. Arrigo. 2007. Potential roles of membrane fluidity and ceramide in hyperthermia and alcohol stimulation of TRAIL apoptosis. *Apoptosis.* 12:1703–1720.
17. Atsumi, G., M. Murakami, M. Tajima, S. Shimbara, N. Hara, et al. 1997. The perturbed membrane of cells undergoing apoptosis is susceptible to type II secretory phospholipase A2 to liberate arachidonic acid. *Biochim. Biophys. Acta.* 1349:43–54.
18. Nielson, K. H., C. A. Olsen, D. V. Allred, K. L. O'Neill, G. F. Burton, et al. 2000. Susceptibility of S49 lymphoma cell membranes to hydrolysis by secretory phospholipase A(2) during early phase of apoptosis. *Biochim. Biophys. Acta.* 1484:163–174.
19. Basse, F., J. G. Stout, P. J. Sims, and T. Wiedmer. 1996. Isolation of an erythrocyte membrane protein that mediates Ca2+- dependent transbilayer movement of phospholipid. *J. Biol. Chem.* 271:17205–17210.
20. Williamson, P., A. Christie, T. Kohlin, R. A. Schlegel, P. Comfurius, et al. 2001. Phospholipid scramblase activation pathways in lymphocytes. *Biochemistry.* 40:8065–8072.
21. Jain, M. K., B. Z. Yu, and A. Kozubek. 1989. Binding of phospholipase A2 to zwitterionic bilayers is promoted by lateral segregation of anionic amphiphiles. *Biochim. Biophys. Acta.* 980:23–32.
22. Yu, B. Z., M. J. Poi, U. A. Ramagopal, R. Jain, S. Ramakumar, et al. 2000. Structural basis of the anionic interface preference and kcat* activation of pancreatic phospholipase A2. *Biochemistry.* 39:12312–12323.
23. Gelb, M. H., M. K. Jain, A. M. Hanel, and O. G. Berg. 1995. Interfacial enzymology of glycerolipid hydrolases: lessons from secreted phospholipases A2. *Annu. Rev. Biochem.* 64:653–688.
24. Singer, A. G., F. Ghomashchi, C. Le Calvez, J. Bollinger, S. Bezzine, et al. 2002. Interfacial kinetic and binding properties of the complete set of human and mouse groups I, II, V, X, and XII secreted phospholipases A2. *J. Biol. Chem.* 277:48535–48549.
25. Berki, T., L. Palinkas, F. Boldizsar, and P. Nemeth. 2002. Glucocorticoid (GC) sensitivity and GC receptor expression differ in thymocyte subpopulations. *Int. Immunol.* 14:463–469.
26. van Engeland, M., H. J. Kuijpers, F. C. Ramaekers, C. P. Reutelingsperger, and B. Schutte. 1997. Plasma membrane alterations and cytoskeletal changes in apoptosis. *Exp. Cell Res.* 235:421–430.
27. Lagerberg, J. W., K. J. Kallen, C. W. Haest, J. VanSteveninck, and T. M. Dubbelman. 1995. Factors affecting the amount and the mode of merocyanine 540 binding to the membrane of human erythrocytes. A comparison with the binding to leukemia cells. *Biochim. Biophys. Acta.* 1235:428–436.
28. Murakami, M., T. Kambe, S. Shimbara, K. Higashino, K. Hanasaki, et al. 1999. Different functional aspects of the group II subfamily (types IIA and V) and type X secretory phospholipase A(2)s in regulating arachidonic acid release and prostaglandin generation. Implications of cyclooxygenase-2 induction and phospholipid scramblase-mediated cellular membrane perturbation. *J. Biol. Chem.* 274:31435–31444.
29. Wilson, H. A., W. Huang, J. B. Waldrip, A. M. Judd, L. P. Vernon, et al. 1997. Mechanisms by which thionin induces susceptibility of S49 cell membranes to extracellular phospholipase A2. *Biochim. Biophys. Acta.* 1349:142–156.
30. Henshaw, J. B., C. A. Olsen, A. R. Farnbach, K. H. Nielson, and J. D. Bell. 1998. Definition of the specific roles of lysolecithin and palmitic acid in altering the susceptibility of dipalmitoylphosphatidylcholine bilayers to phospholipase A2. *Biochemistry.* 37:10709–10721.
31. Burack, W. R., Q. Yuan, and R. L. Biltonen. 1993. Role of lateral phase separation in the modulation of phospholipase A2 activity. *Biochemistry.* 32:583–589.
32. Smith, S. K., A. R. Farnbach, F. M. Harris, A. C. Hawes, L. R. Jackson, et al. 2001. Mechanisms by which intracellular calcium induces susceptibility to secretory phospholipase A2 in human erythrocytes. *J. Biol. Chem.* 276:22732–22741.
33. Harris, F. M., S. K. Smith, and J. D. Bell. 2001. Physical properties of erythrocyte ghosts that determine susceptibility to secretory phospholipase A2. *J. Biol. Chem.* 276:22722–22731.
34. Burack, W. R., A. R. Dibble, M. M. Allietta, and R. L. Biltonen. 1997. Changes in vesicle morphology induced by lateral phase separation modulate phospholipase A2 activity. *Biochemistry.* 36:10551–10557.
35. Tatulian, S. A. 2001. Toward understanding interfacial activation of secretory phospholipase A2 (PLA2): membrane surface properties and membrane-induced structural changes in the enzyme contribute synergistically to PLA2 activation. *Biophys. J.* 80:789–800.
36. Hoyrup, P., T. H. Callisen, M. O. Jensen, A. Halperin, and O. G. Mouritsen. 2004. Lipid protrusions, membrane softness, and enzymatic activity. *Phys. Chem. Chem. Phys.* 6:1608–1615.
37. Jensen, L. B., N. K. Burgess, D. D. Gonda, E. Spencer, H. A. Wilson-Ashworth, et al. 2005. Mechanisms governing the level of susceptibility of erythrocyte membranes to secretory phospholipase A2. *Biophys. J.* 88:2692–2705.
38. Vest, R., R. Wallis, L. B. Jensen, A. C. Haws, J. Callister, et al. 2006. Use of steady-state laurdan fluorescence to detect changes in liquid ordered phases in human erythrocyte membranes. *J. Membr. Biol.* 211:15–25.
39. Best, K. B., A. J. Ohran, A. C. Hawes, T. L. Hazlett, E. Gratton, et al. 2002. Relationship between erythrocyte membrane phase properties and susceptibility to secretory phospholipase A2. *Biochemistry.* 41:13982–13988.
40. Arnold, R., D. Brenner, M. Becker, C. R. Frey, and P. H. Krammer. 2006. How T lymphocytes switch between life and death. *Eur. J. Immunol.* 36:1654–1658.
41. Martin, S. J., D. M. Finucane, G. P. Amarante-Mendes, G. A. O'Brien, and D. R. Green. 1996. Phosphatidylserine externalization during CD95-induced apoptosis of cells and cytoplasts requires ICE/CED-3 protease activity. *J. Biol. Chem.* 271:28753–28756.
42. LeDuc, P. P., and R. R. Bellin. 2006. Nanoscale intracellular organization and functional architecture mediating cellular behavior. *Ann. Biomed. Eng.* 34:102–113.
43. Coleman, M. L., and M. F. Olson. 2002. Rho GTPase signalling pathways in the morphological changes associated with apoptosis. *Cell Death Differ.* 9:493–504.
44. Cybulsky, A. V., T. Takano, J. Papillon, A. Khadir, K. Bijian, et al. 2004. The actin cytoskeleton facilitates complement-mediated activation of cytosolic phospholipase A2. *Am. J. Physiol. Renal Physiol.* 286:F466–F476.
45. Panebra, A., S. X. Ma, L. W. Zhai, X. T. Wang, S. G. Rhee, et al. 2001. Regulation of phospholipase C-gamma(1) by the actin-regulatory protein villin. *Am. J. Physiol. Cell Physiol.* 281:C1046–C1058.

46. Kusner, D. J., J. A. Barton, K. K. Wen, X. Wang, P. A. Rubenstein, et al. 2002. Regulation of phospholipase D activity by actin. Actin exerts bidirectional modulation of mammalian phospholipase D activity in a polymerization-dependent, isoform-specific manner. *J. Biol. Chem.* 277:50683–50692.

47. Wilson, H. A., J. B. Waldrip, K. H. Nielson, A. M. Judd, S. K. Han, et al. 1999. Mechanisms by which elevated intracellular calcium induces S49 cell membranes to become susceptible to the action of secretory phospholipase A2. *J. Biol. Chem.* 274:11494–11504.

48. Remy-Kristensen, A., G. Duportail, G. Coupin, and J. G. Kuhry. 2000. The influence of microtubule integrity on plasma membrane fluidity in L929 cells. *Mol. Membr. Biol.* 17:95–100.

49. Gaus, K., E. Chklovskaia, G. B. Fazekas de St, W. Jessup, and T. Harder. 2005. Condensation of the plasma membrane at the site of T lymphocyte activation. *J. Cell Biol.* 171:121–131.

50. Taha, T. A., T. D. Mullen, and L. M. Obeid. 2006. A house divided: ceramide, sphingosine, and sphingosine-1-phosphate in programmed cell death. *Biochim. Biophys. Acta.* 1758:2027–2036.

51. Chiantia, S., N. Kahya, J. Ries, and P. Schwille. 2006. Effects of ceramide on liquid-ordered domains investigated by simultaneous AFM and FCS. *Biophys. J.* 90:4500–4508.

52. Silva, L. C., R. F. de Almeida, B. M. Castro, A. Fedorov, and M. Prieto. 2007. Ceramide-domain formation and collapse in lipid rafts: membrane reorganization by an apoptotic lipid. *Biophys. J.* 92:502–516.

53. Maderna, P., and C. Godson. 2003. Phagocytosis of apoptotic cells and the resolution of inflammation. *Biochim. Biophys. Acta.* 1639: 141–151.

54. Krysko, D. V., T. Vanden Berghe, K. D'Herde, and P. Vandenabeele. 2008. Apoptosis and necrosis: detection, discrimination and phagocytosis. *Methods.* 44:205–221.